Cu_2MSiO_5 (M = Co, Ni): A new silicate material with chains of Cu and M ions

S. W. Lee,[1] H. Guo,[1] L. Zhao,[1] Z. Hu,[1] T. Mueller,[2] H. J. Lin,[3] C. T. Chen,[3] G. Ryu,[1,4] L. H. Tjeng,[1] and A. C. Komarek[1,*]

[1]*Max-Planck-Institute for Chemical Physics of Solids, Nöthnitzer Straße 40, D-01187 Dresden, Germany*

[2]*Forschungszentrum Jülich GmbH, Jülich Centre for Neutron Science (JCNS) at Heinz Maier-Leibnitz Zentrum (MLZ), Lichtenbergstraße 1, 85748 Garching, Germany*

[3]*National Synchrotron Radiation Research Center (NSRRC), 101 Hsin-Ann Road, Hsinchu 30076, Taiwan*

[4]*Max-Planck-POSTECH Center for Complex Phase Materials, Pohang University of Science and Technology, Pohang 37673, Korea*

(Received 15 November 2018; published 20 March 2019)

We report on the synthesis of a new material with a novel quasi-one-dimensional crystal structure consisting of chains of Cu and M ions: Cu_2MSiO_5 with M = Co, Ni. Large, centimeter-sized single crystals of Cu_2CoSiO_5 have been grown by the floating-zone technique and roughly hexagonally shaped single crystals of Cu_2NiSiO_5 have been grown by means of chemical vapor transport. Cu_2CoSiO_5 (Cu_2NiSiO_5) orders antiferromagnetically below $T_N \sim 15$ K (12.5 K). Polarized neutron scattering experiments on Cu_2CoSiO_5 reveal incommensurate magnetism below T_N with propagation vectors $\mathbf{k}^{\pm} = \pm(\sim 0.2\ 0\ 0.3)$, and magnetic susceptibility measurements indicate a large unquenched orbital moment of about 1 μ_B per Co ion.

DOI: 10.1103/PhysRevMaterials.3.034408

I. INTRODUCTION

Silicon dioxide SiO_2 in form of quartz is the second most abundant mineral in the continental crust of the earth. It consists of covalently bound Si-oxygen tetrahedra that are also the building blocks of a wide variety of other silicate minerals which are the major compounds of the earths crust. This demonstrates the importance of silicates for mineralogy, where silicates are classified in groups depending on the interconnection of the Si-O tetrahedra within the structure: nesosilicates with isolated $[SiO_4]^{4\ominus}$ tetrahedra, sorosilicates with $[Si_mO_{3m+1}]^{(2m+2)\ominus}$ tetrahedral groups, cyclosilicates froming $[Si_nO_{3n}]^{2n\ominus}$ rings, inosilicates forming $[Si_pO_{3p}]^{2p\ominus}$ chains or $[Si_{4n}O_{11n}]^{6n\ominus}$ double chains etc., phyllosilicates with Si-O tetrahedral single or double sheets, and tectosilicates (with Al for charge balance) forming a fully three-dimensional (Si,Al)-O tetrahedral network. Besides their importance for mineralogy, silicates are also of interest for industry since they belong to the most important ingredients of concrete or cement. Especially, tricalcium silicate Ca_3SiO_5 (alite) is a main constituent of Portland cement [1]. Recently, silicates that possess magnetic ions have also attracted considerable attention due to the occurrence of multiferroicity in these systems, which is of interest for future electric devices. For example, the clinopyroxene $NaFeSi_2O_6$ (aegirine) which belongs to the class of single chain inosilicates exhibits ferroelectricity within a magnetically ordered state with incommensurate magnetic order [2,3]. Such incommensurate magnetic order might directly induce the ferroelectric polarization instead of accidentally coexisting with it, as in formerly known multiferroics [4,5]. Thus, the ferroelectric properties in these magnetoelectric multiferroics might be controlled by magnetism and vice versa, which could be exploited in future electronic devices [6].

Here, we report of the synthesis of a new nesosilicate material, Cu_2MSiO_5, with a novel quasi-one-dimensional (1D) crystal structure consisting of chains of Cu and M ions. This compound can be obtained formally by exchanging the three divalent and nonmagnetic Ca^{2+} ions in alite by isovalent but distinctly smaller and magnetic transition metal ions Cu^{2+} and $M = Co^{2+}, Ni^{2+}$. The magnetic transition metal ions in Cu_2CoSiO_5 (Cu_2NiSiO_5) order antiferromagnetically below $T_N \sim 15$ K ($\sim$12.5 K). Polarized neutron scattering experiments on Cu_2CoSiO_5 reveal an incommensurate magnetic order with the propagation vectors $\mathbf{k}^{\pm} = \pm(\sim 0.2\ 0\ 0.3)$.

II. EXPERIMENT

The centimeter sized Cu_2CoSiO_5 single crystal shown in Fig. 1(a) was grown in a Crystal Systems Corp. (CSC) optical floating-zone furnace equipped with four elliptical mirrors. The initial polycrystalline rods were prepared from stoichiometric amounts of $CoCO_3$, SiO_2, and CuO. The mixed starting materials were sintered in air at 850 °C for 72 hours with several intermediate grindings. Finally, the ground powder was pressed under a hydrostatic pressure of $\sim$40 MPa into a rod with $\sim$8 mm in diameter and $\sim$15 cm in length which was sintered for 24 hours at 900 °C in air. The floating-zone growth was performed in an oxygen atmosphere of 2.6 bar pressure with a growth speed of 2.25 mm/h with counter-rotating feed and seed rods ($\sim$5 rpm).

Cu_2NiSiO_5 single crystals were grown by chemical vapor transport in an evacuated quartz ampoule with an applied temperature gradient. For these purposes 0.5 g of Cu_2NiSiO_5 powder was sealed in an evacuated quartz ampoule (together with $\sim$50 mg of $TeCl_4$ and $\sim$50 mg of AgF_2). The reaction was performed in a three-zone furnace with the quartz ampoule extending over two zones heated to temperatures of $T_{1,3} = 750$ °C and $T_2 = 850$ °C.

For powder x-ray diffraction (XRD) measurements, parts of the grown single crystals were ground to powder. The

*Alexander.Komarek@cpfs.mpg.de

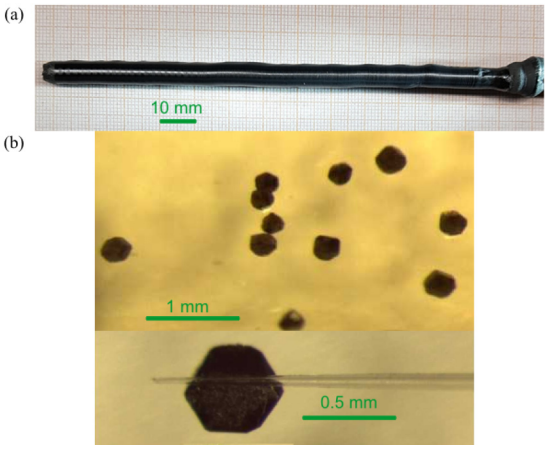

FIG. 1. Photos of (a) the floating-zone grown Cu_2CoSiO_5 single crystal and (b) typical Cu_2NiSiO_5 single crystals grown by chemical vapor transport.

XRD measurements were performed on a Bruker D8 DISCOVER A25 powder x-ray diffractometer. The FULLPROF program package [7] was used for Rietveld refinements. Neutron scattering experiments were performed at the DNS spectrometer [8,9] at the Heinz Maier–Leibnitz Zentrum using an incident neutron wavelength of $\lambda = 4.2$ Å. a^*, b^*, and c^* are defined as reciprocal lattice vectors in this article, i.e., $\mathbf{a}^* = 2\pi \cdot (\mathbf{b} \times \mathbf{c})/(\mathbf{a} \circ \mathbf{b} \times \mathbf{c})$, etc. In the following all units are given in these reciprocal lattice units (r.l.u.).

Using Mo $K\alpha$ radiation, single-crystal x-ray diffraction measurements were performed on a Bruker D8 VENTURE

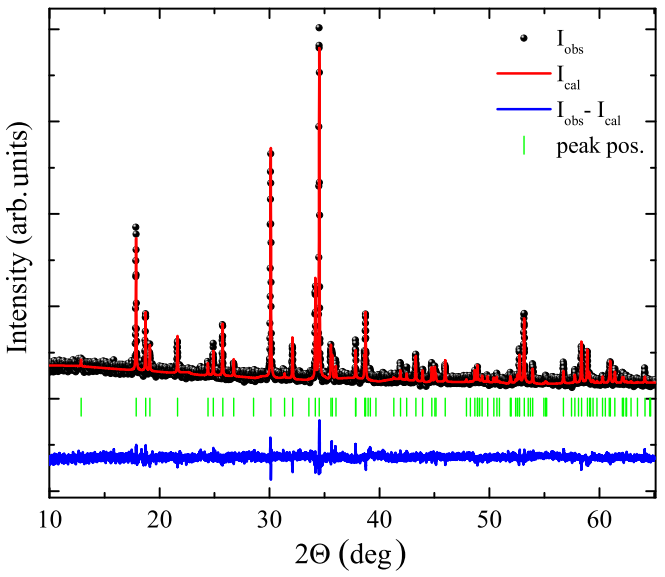

FIG. 2. Room temperature powder x-ray diffraction pattern of a powder obtained from a piece of the floating-zone grown Cu_2CoSiO_5 single crystal. The black dots represent the observed intensities I_{obs}; the solid red line represents the calculated Intensities I_{cal} obtained from a Rietveld fit based on the crystal structure determined by single crystal X-ray diffraction (in Fig. 4). The solid blue line and the vertical bars represent $I_{obs} - I_{cal}$ and the calculated Bragg peak positions respectively.

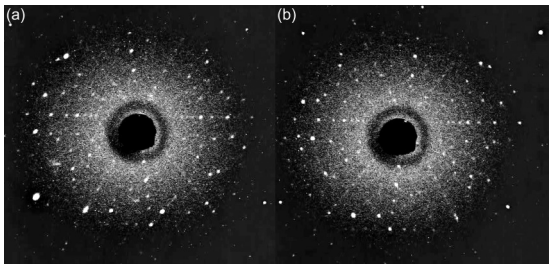

FIG. 3. Laue Photos of (a) front side and (b) back side of a floating-zone grown Cu_2CoSiO_5 single crystal.

single-crystal x-ray diffractometer equipped with a bent graphite monochromator for about 3× intensity enhancement and a Bruker PHOTON CMOS large area detector.

The soft x-ray absorption spectra at the Co-$L_{2,3}$ and Cu-$L_{2,3}$ edges of Cu_2CoSiO_5 and CoO as a Co^{2+} reference and CuO (Cu_2O) as a Cu^{2+} (Cu^{1+}) reference, respectively, were measured at the 11A beamline at the National Synchrotron Radiation Research Center (NSRRC) in Taiwan using the total electron yield method.

TABLE I. Refinement results of single-crystal x-ray diffraction measurements of Cu_2CoSiO_5. Here, the structural parameters of the refinement with space group $C12/m1$ ($a = 9.4231$ Å, $b = 6.2707$ Å, $c = 7.9359$ Å, $\beta = 118.6308°$) are listed. Goodness of fit, R, and weighted R values amount to 2.14, 1.59%, and 5.78% respectively.

Atom	x	y	z
Cu1	0.25	− 0.25	0
Cu2	− 0.11206(3)	− 0.5	− 0.20056(3)
Co1	0	− 0.23746(4)	− 0.5
Si1	0.22282(6)	0	− 0.65341(7)
O1	− 0.1103(2)	− 0.5	− 0.4411(2)
O2	0.1282(2)	− 0.5	− 0.0329(2)
O3	0.0629(2)	0	− 0.6275(2)
O4	0.2455(1)	− 0.2159(2)	0.2478(2)
Atom	U_{11} (Å^2)	U_{22} (Å^2)	U_{33} (Å^2)
Cu1	0.0098(1)	0.00605(9)	0.0080(1)
Cu2	0.00796(9)	0.0123(1)	0.00549(9)
Co1	0.0076(1)	0.00487(9)	0.0107(1)
Si1	0.0059(2)	0.0048(2)	0.0059(2)
O1	0.0073(4)	0.0152(5)	0.0066(4)
O2	0.0062(4)	0.0075(4)	0.0069(4)
O3	0.0086(5)	0.0089(5)	0.0131(5)
O4	0.0201(5)	0.0069(3)	0.0150(4)
Atom	U_{12} (Å^2)	U_{13} (Å^2)	U_{23} (Å^2)
Cu1	− 0.00192(6)	0.00616(8)	− 0.00144(5)
Cu2	0	0.00395(7)	0
Co1	0	0.00620(8)	0
Si1	0	0.0037(1)	0
O1	0	0.0035(4)	0
O2	0	0.0039(4)	0
O3	0	0.0075(4)	0
O4	− 0.0031(3)	0.0140(4)	− 0.0032(3)

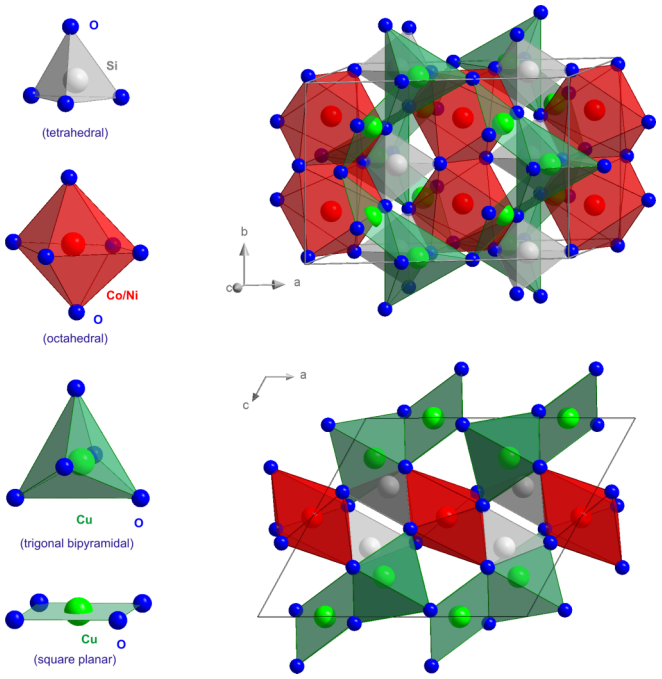

FIG. 4. Crystal structure of Cu_2MSiO_5 (M = Co, Ni). The oxygen coordination of the metal ions is shown on the left side, and the unit cell of Cu_2MSiO_5 for two different viewing directions (perpendicular and parallel to the chains running in the b direction) is shown on the upper and lower right.

The magnetization was measured using a superconducting quantum interference device (SQUID) magnetometer (MPMS, Quantum Design).

III. RESULTS AND DISCUSSION

A. Cu_2CoSiO_5

Powder x-ray diffraction measurements indicate that our floating-zone grown single crystal shown in Fig. 1(a) is free from any impurities; see Fig. 2. The untwined single crystalline nature of our centimeter-sized Cu_2CoSiO_5 single crystal was ascertained by single-crystal x-ray, neutron,

TABLE II. R and weighted R values obtained in structural refinements of Cu_2CoSiO_5 and Cu_2NiSiO_5 with different crystal structure models where the Co or Ni ions are located at one of the other Cu sites.

Cu_2CoSiO_5				
Octahedral	Trigonal bipyramidal	Square planar	R value	R_w value
Co	Cu	Cu	1.59%	5.78%
Cu	Co	Cu	4.39%	16.34%
Cu	Cu	Co	6.80%	23.18%
Cu_2NiSiO_5				
Octahedral	Trigonal bipyramidal	Square planar	R value	R_w value
Ni	Cu	Cu	1.62%	4.85%
Cu	Ni	Cu	2.89%	9.21%
Cu	Cu	Ni	3.16%	11.76%

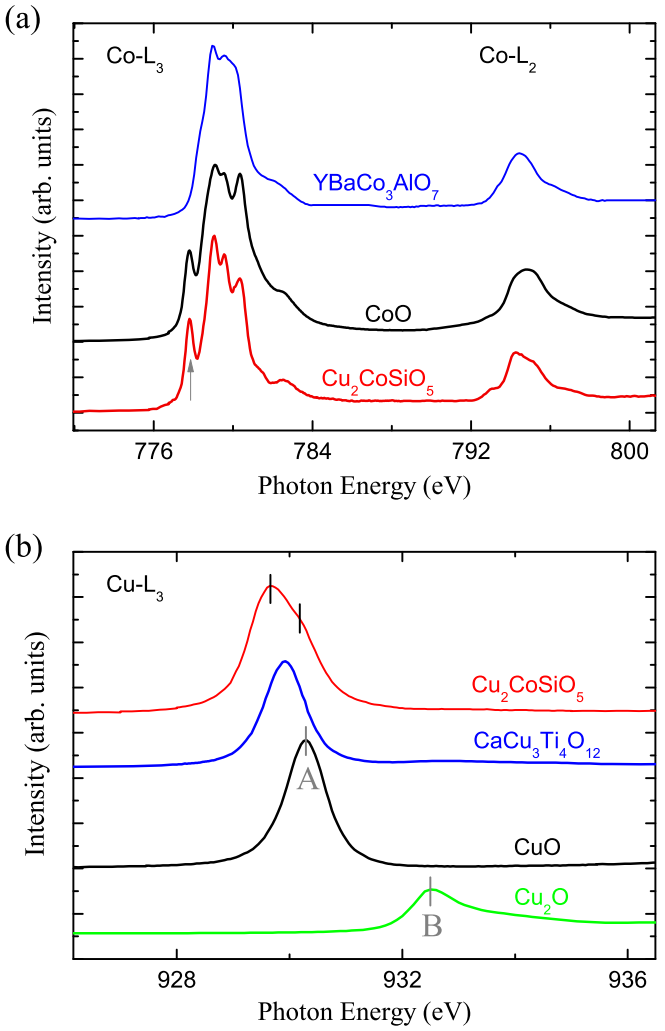

FIG. 5. (a) The Co-$L_{2,3}$ XAS spectra of Cu_2CoSiO_6 and CoO with Co^{2+} ions in an octahedral coordination and $YBaCo_3AlO_7$ (from Ref. [12]) with Co^{2+} in a tetrahedral coordination. (b) The Cu-L_3 XAS spectra of Cu_2CoSiO_5 and of Cu_2O, CuO, and $CaCu_3Ti_4O_{12}$ (from Ref. [16]) for comparison.

and Laue diffraction techniques; see Fig. 3. An untwined Cu_2CoSiO_5 single crystal was measured by means of single-crystal x-ray diffraction up to $2\Theta_{max} = 90°$, and a multiscan absorption correction was applied to the data (minimum and maximum transmissions of 0.5150 and 0.7488 respectively). 21 078 observed reflections (h: $-18 \rightarrow 18$; k: $-12 \rightarrow 12$; and l: $-15 \rightarrow 15$) were collected with an internal R value of 3.11%, a redundancy of 14.4, and 99.94% coverage up to $\sin(\Theta)/\lambda = 0.988$. The crystal structure of this new compound was solved using the JANA 2006 software package [10,11]. The obtained structural parameters are listed in Table I.

The crystal structure of the new silicate Cu_2CoSiO_5 is shown in Fig. 4. The arrangement of the isolated SiO_4 tetrahedra resembles the one inside the unit cell of alite (Ca_3SiO_5), which also exists in a monoclinic form [$a = 12.235(3)$ Å, $b = 7.073(2)$ Å, $c = 9.298(3)$ Å, $\beta = 116.31(5)°$]. Instead of CaO_6 octahedra the space between the SiO_4 tetrahedra in the nesosilicate Cu_2CoSiO_5 is filled with three different

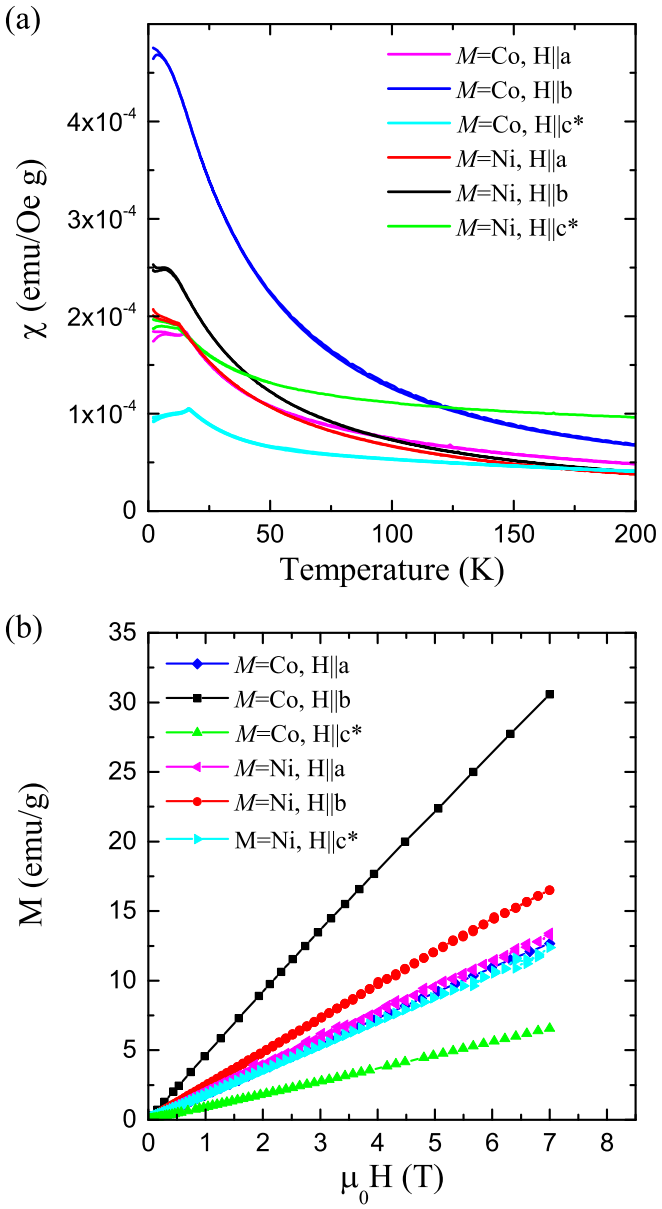

FIG. 6. (a) Temperature dependence of the magnetic susceptibility of Cu_2MSiO_5 (M = Co, Ni) for field-cooled and zero-field-cooled measurement conditions in magnetic fields of $\mu_0 H = 0.1$ and 0.25 T for M = Co and Ni respectively. The field was applied along the crystallographic a and b directions as well as the c^* direction, which is perpendicular to a and b within this monoclinic system ($a \perp b \perp c^*$). (b) Magnetization measurements of Cu_2MSiO_5 at 2 K.

motifs or building blocks—CoO_6 octahedra, CuO_5 trigonal bipyramids, and square planar CuO_4 plaquettes—which results in the observed crystal structure. Edge-sharing chains of CoO_6 octahedra run in the b direction. Between these chains, corner-sharing CuO_4 plaquettes form zig-zag chains which also run in the b direction. And, single CuO_5 trigonal bipyramids (and SiO_4 tetrahedra) fill the space between these two kind of chains; see Fig. 4. In order to verify that the Co^{2+} ions are located at the octahedral sites, we tried also refinements with the Co ions located at square planar or trigonal bipyramidal sites. However, the refinement becomes significantly worse for these alternative structure models, see Table II, thus confirming our structure model with copper ions located at square planar and trigonal bipyramidal coordinated sites and cobalt ions situated at octahedrally coordinated sites (Fig. 4 and Table I).

In order to confirm these local environments of the Cu and Co ions as well as their valence states in Cu_2CoSiO_5, soft x-ray absorption spectroscopy (XAS) at the Co-$L_{2,3}$ and Cu-$L_{2,3}$ edges was performed. It is well known that the Co-$L_{2,3}$ XAS spectrum is sensitive to the valence state of the Co ion: an increase of the valence state of the Co ion by 1 causes a shift of the XAS $L_{2,3}$ spectra by 1 or more eV toward higher energies [12,13]. The Co-$L_{2,3}$ XAS spectrum of Cu_2CoSiO_5 in Fig. 5(a) is located at the same energy position as that of CoO, demonstrating the Co^{2+} state. We would like to emphasize here that the multiplet spectral structures in the 3d transition metal $L_{2,3}$ edges are highly sensitive to the local environments of transition metal ions [12,14,15]. For comparison we presents two Co^{2+} references in Fig. 5(a): one with an octahedral local symmetry, i.e., CoO, and one with a tetrahedral local symmetry, i.e., $YBaCo_3AlO_7$ (from Ref. [12]). The similar multiplet spectral features of Cu_2CoSiO_5 and CoO, especially the sharp lower energy peak at 777.8 eV that is a fingerprint of Co^{2+} ions in octahedral coordination [14,15], clearly indicate that the Co^{2+} ions in Cu_2CoSiO_5 have an octahedral oxygen environment.

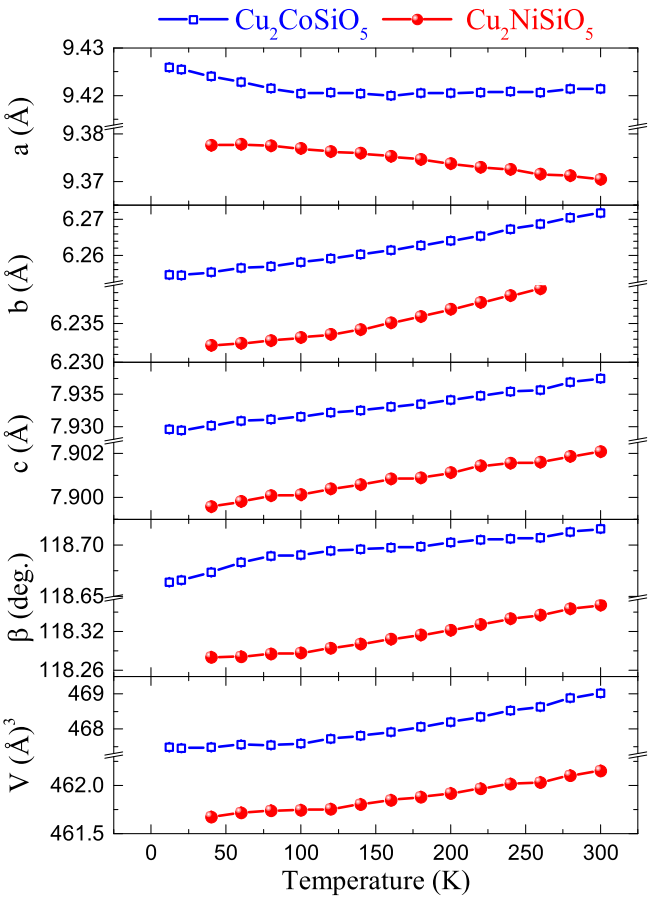

FIG. 7. Lattice constants of Cu_2CoSiO_5 (blue squares) and Cu_2NiSiO_5 (red dots) as a function of temperature.

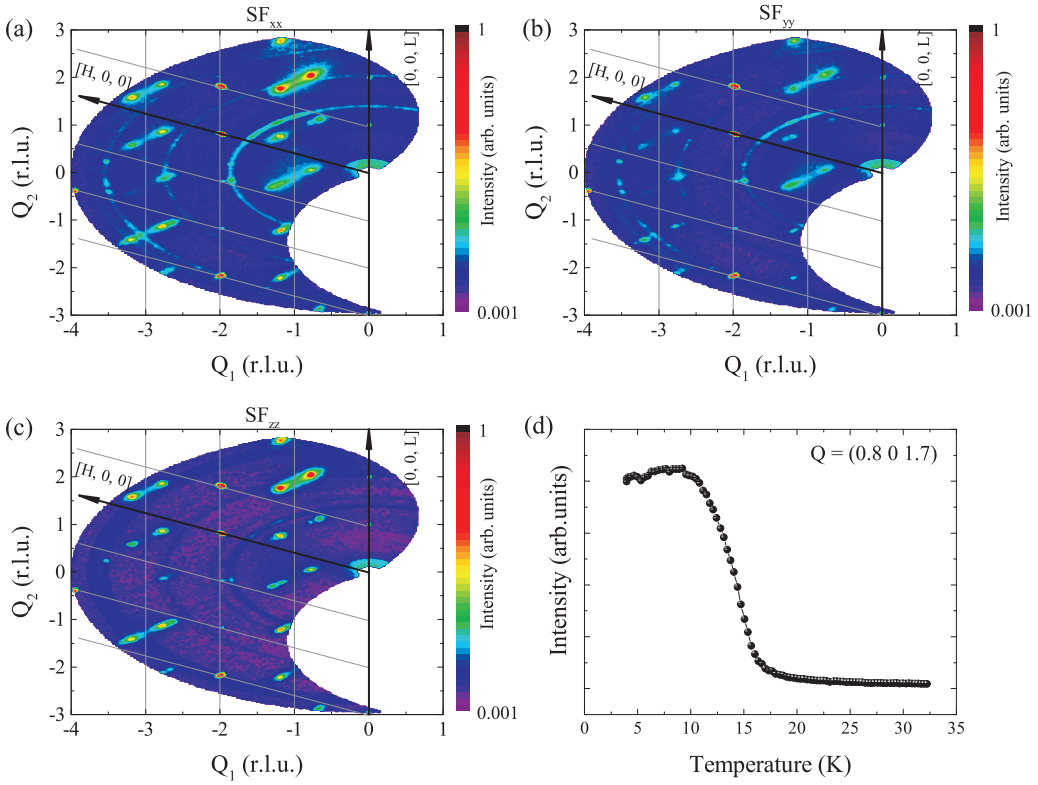

FIG. 8. Polarized neutron measurements of a Cu_2CoSiO_5 single crystal. (a)–(c) The neutron scattering intensities within the spin-flip channels (a) SF$_{xx}$, (b) SF$_{yy}$, and (a) SF$_{zz}$ detected within the reciprocal plane spanned by $\mathbf{Q_1} = (-1\ 0\ 0.4)$ and $\mathbf{Q_2} = (0\ 0\ 1)$. Here, the x, y, and z directions are parallel to the average $\mathbf{Q}$, and perpendicular to the average $\mathbf{Q}$ within the scattering plane and out of the scattering plane, respectively. The flipping ratio amounts to ∼25 and intensities were not corrected for imperfect neutron polarization. Note, that the DNS spectrometer has a relaxed resolution in out-of-plane (here: K) direction. (d) The temperature dependence of a (0.8 0 1.7) magnetic peak measured in the SF$_{xx}$ channel.

After confirming the octahedral coordination of the Co^{2+} ions, we further examineed the valence and local coordination of the Cu ions. Figure 5(b) shows the Cu-L_3 edge of Cu_2CoSiO_5 and Cu_2O as Cu^{1+} reference, and CuO and $CaCu_3Ti_4O_{12}$ (from Ref. [16]) as Cu^{2+} references. The strong white line A at 930.3 eV in the Cu-$L_{2,3}$ XAS spectrum of CuO stands for a $2p^53d^{10}$ final state of the Cu^{2+} ions, while the weak broad feature B at 932.4 eV is assigned to a $2p^53d^{10}4s^1$ final state of the Cu^{1+} ions [17]. The Cu peak in Cu_2CoSiO_5 has a very strong intensity, like that in CuO, and its energy position is very close to that of CuO, so that we can safely conclude that the Cu ions in Cu_2CoSiO_5 are in the divalent state. Comparing CuO with $CaCu_3Ti_4O_{12}$, we can observe that the Cu-L_3 peak in CuO appears at a higher energy, by about 0.4 eV. Realizing that the average square planar Cu-O bond distance in CuO (1.9543 Å from 2 × 1.9481 Å and 2 × 1.9606 Å) is somewhat smaller than that in $CaCu_3Ti_4O_{12}$ (1.9671 Å from 4 × 1.9671 Å), we may attribute the higher energy of the CuO peak to be associated with the stronger covalency. The main peak of the Cu-L_3 XAS spectrum of Cu_2CoSiO_5 has two components, at 0.6 and 0.2 eV below that of CuO. The average Cu-O bond distance in the trigonal bipyramidal sites is about 2.0132 Å (from 1.9306, 2.0026, 1.9170, and 2 × 2.1079 Å) while that in the square planar sites amounts to 1.9420 Å (from 2 × 1.8855 Å and 2 × 1.9986 Å). It is therefore tempting to suggest that the lowest energy peak originates from the trigonal bipyramidal sites while the higher energy peak is due to the square planar coordinated Cu sites.

Furthermore, we would like to remark that the oxygen coordination of the copper ions in Cu_2MSiO_5 resembles the oxygen coordination in the skyrmion hosting material Cu_2OSeO_3, which has attracted considerable attention recently [18–21]. Also in Cu_2OSeO_3 copper is locally coordinated by oxygen in a way such that CuO_5 bipyramids and CuO_4 plaquettes are formed [22] as in Cu_2MSiO_5.

The temperature dependence of the magnetic susceptibility χ of Cu_2CoSiO_5 is shown in Fig. 6(a). An antiferromagnetic transition at $T_N \sim 15$ K becomes apparent on cooling to lowest temperatures. A Curie-Weiss fit of the magnetic susceptibility reveals an effective moment which amounts to 5.65 μ_B/f.u. Based on the assumption that the effective moment per Cu^{2+} ion is 1.73 μ_B with $S = 1/2$ and $g = 2$, the effective moment per Co^{2+} ion amounts to about 5.1 μ_B. Since the spin-only effective moment for the Co^{2+} with $S = 3/2$ is 3.87 μ_B, the presence of a sizable unquenched orbital moment of the Co^{2+} ions can be expected, of the order of 1 μ_B per Co ion. The Curie-Weiss temperatures Θ_{CW} are in general distinctly larger than the observed magnetic ordering temperature, thus indicating a large degree of frustration in this compound. The values of Θ_{CW} amount to −97.3(3), −21.9(2), and −225.1(2) K for the a, b, and c^* directions. The much smaller value along the crystallographic b direction in-

dicates, in total, much weaker antiferromagnetic interactions in chain direction. This would be consistent with a scenario where some of these chains have a ferromagnetic intrachain interaction. However, there is no sign of magnetic low dimensionality in the temperature dependence of the magnetic susceptibility, such as a hump-like feature above T_N which might due to a coupling of Cu and Co ions in neighboring chains. As expected for this antiferromagnetic compound, also the magnetization of Cu_2CoSiO_5 is almost linear up to 7 T; see Fig. 6(b).

Using a high resolution powder x-ray diffractometer, we measured the temperature dependence of the lattice parameters of Cu_2CoSiO_5; see Fig. 7. As can be seen, there is an anomalous increase of the a lattice constant on cooling below about 100 K which occurs well above the magnetic ordering temperature of Cu_2CoSiO_5. This anomalous behavior might have entirely structural origins since the magnetic ordering temperature of Cu_2CoSiO_5 is much lower.

Finally, incommensurate magnetic peaks appearing below T_N have been observed in polarized neutron scattering experiments on a Cu_2CoSiO_5 single crystal by mapping large regions in reciprocal space; see Figs. 8(a)–8(c). The temperature dependence of such a magnetic peak is shown in Fig. 8(d). Hence, the quasi-1D material Cu_2CoSiO_5 exhibits incommensurate magnetism below $T_N \sim 15$ K with the propagation vectors $\mathbf{k}^{\pm} = \pm(\sim 0.2\ 0\ 0.3)$. The appearance of incommensurate magnetism might be a consequence of frustration in this quasi-1D system. Frustration might arise especially from the interconnection of CoO_3 octahedral chains and CuO_2 zig-zag chains via isolated CuO_5 trigonal bipyramids that introduce additional exchange interactions. The propagation vector without the b^* component indicates that the modulation appears between (and not within) the quasi-1D chains. Hence, the magnetic moments within the chains of the copper-oxygen plaquettes running in the b direction are probably ferromagnetically ordered. This would also be in agreement with a sharp Cu-O-Cu bond angle within the corner-sharing CuO_2 zig-zag chains which amounts to $\sim$112.5°. Also the Co-O-Co bond angle within the edge-sharing CoO_3 octahedral chains is close to 93.7°. The strongest magnetic signal appears in the spin-flip SF_{xx} and SF_{zz} channels and the signal is almost absent in the SF_{yy} channel, thus indicating that the moments are aligned within the ac plane, i.e., perpendicular to the chains.

B. Cu_2NiSiO_5

We grew almost hexagonal shaped Cu_2NiSiO_5 single crystals by means of chemical vapor transport; see Fig. 1(b). One of these Cu_2NiSiO_5 single crystals was measured by means of single-crystal x-ray diffraction (12 085 reflections collected up to $2\Theta_{max} = 104.2°$; h: $-20 \rightarrow 20$; k: $-13 \rightarrow 13$; and l: $-17 \rightarrow 17$, with an internal R value of 3.20% and a redundancy of 6.4). The resulting structural parameters of the crystal structure are listed in Table III. Also for the nickel copper silicate the Ni^{2+} ions are situated in an octahedral environment like the Co ions in Cu_2CoSiO_5, as is revealed by the comparison of different structure models with Ni ions located at other than octahedral sites that yield worse R and weighted R values; see Table II. Hence, the Co ions in Cu_2CoSiO_5 can be substituted by Ni ions.

TABLE III. Structural parameters of Cu_2NiSiO_5 obtained by means of single-crystal x-ray diffraction: space group $C12/m1$, $a = 9.4415$ Å, $b = 6.2582$ Å, $c = 7.9329$ Å, $\beta = 118.3782°$. Goodness of fit, R and weighted R values are 1.58, 1.62%, and 4.85% respectively.

Atom	x	y	z
Cu1	0.25	0.75	0
Cu2	−0.11196(3)	−0.5	−0.20021(3)
Ni1	0	0.76133(3)	0.5
Si1	0.22276(6)	0	−0.65240(7)
O1	−0.1093(2)	−0.5	−0.4409(2)
O2	0.1282(2)	−0.5	−0.0325(2)
O3	0.0642(2)	0	−0.6229(2)
O4	0.2443(1)	−0.2154(2)	0.2475(2)
Atom	U_{11} (Å^2)	U_{22} (Å^2)	U_{33} (Å^2)
Cu1	0.0115(1)	0.00608(9)	0.00878(9)
Cu2	0.00864(9)	0.0127(1)	0.00568(9)
Ni1	0.0079(1)	0.00592(9)	0.0099(1)
Si1	0.0072(2)	0.0047(2)	0.0060(2)
O1	0.0076(5)	0.0179(6)	0.0070(5)
O2	0.0074(5)	0.0070(4)	0.0078(4)
O3	0.0085(5)	0.0092(5)	0.0128(5)
O4	0.0302(6)	0.0074(3)	0.0208(5)
Atom	U_{12} (Å^2)	U_{13} (Å^2)	U_{23} (Å^2)
Cu1	−0.00215(6)	0.00734(8)	−0.00164(6)
Cu2	0	0.00435(7)	0
Ni1	0	0.00585(8)	0
Si1	0	0.0043(2)	0
O1	0	0.0039(4)	0
O2	0	0.0048(4)	0
O3	0	0.0072(4)	0
O4	−0.0055(3)	0.0217(5)	−0.0053(3)

Moreover, the magnetic susceptibility and magnetization measurements of Cu_2NiSiO_5 are shown in Fig. 6. With $T_N \sim 12.5$ K the antiferromagnetic ordering temperature of Cu_2NiSiO_5 is somewhat lower than that of Cu_2CoSiO_5, but of similar size. From a Curie-Weiss fit of the magnetic susceptibility, the extracted effective moment in Cu_2NiSiO_5 amounts to 4.54 μ_B/f.u. Assuming that the effective moment per Cu^{2+} ion amounts to 1.73 μ_B with $S = 1/2$ and $g = 2$, one can extract the effective moment per Ni^{2+} ion, which amounts to about 3.82 μ_B. This value is close to the expected spin-only effective moment of 3.46 μ_B for a Ni^{2+} ion with $S = 1$. Hence, only for $M =$ Co a sizable unquenched orbital moment has been observed in Cu_2MSiO_5. The values of the Curie-Weiss-temperatures Θ_{CW} amount to −31.9(1), −21.1(1), and −28(1) K for the crystallographic a, b, and c^* directions. The values of Θ_{CW} are much more similar for the $M =$ Ni material, which might be due to a different size of competing exchange interactions in this system, thus resulting in less frustration than observed for the $M =$ Co compound. Also for Cu_2NiSiO_5 there appears no hump with a local maximum in the magnetic susceptibility above T_N. Probably, there are also intrachain interactions between the Cu and M ions in the Cu_2MSiO_5 system which lift the magnetic quasi-one-dimensionality in this system that consists of adjacent copper chains and

M-metal chains and would be otherwise also magnetically quasi-one-dimensional. The magnetic low-dimensionality might be gained or enhanced by the substitution of one of these magnetic metal ions in Cu_2MSiO_5 by nonmagnetic ions, which might be a task for future studies.

Finally, the temperature-dependent lattice parameters of Cu_2NiSiO_5 are shown in Fig. 7. As can be seen, there is an anomalous increase of the a lattice constant on cooling within the whole measured temperature range. Thus, this anomalous temperature dependence of the a lattice parameter might be an entirely structural effect. Hence, also for Cu_2CoSiO_5 the anomalous increase of the a lattice parameter below ∼100 K might have an entirely structural origin.

IV. CONCLUSION

In summary, we synthesized a new silicate material Cu_2MSiO_5 with magnetic transition metal ions Cu and M = Co or Ni. Cu_2CoSiO_5 crystallizes in a new quasi-1D crystal structure consisting of silicon-oxygen tetrahedra, cobalt-oxygen octahedra, and copper-oxygen trigonal bipyramids as well as square planar copper-oxygen plaquettes. In this structure, edge-sharing cobalt-oxygen octahedra (corner sharing copper-oxygen plaquettes) form chains (zig-zag-chains) which run in the b direction. The Co-O-Co and Cu-O-Cu bond angles away from 180° (i.e., 93.7° and ∼112.5°, respectively) are indicative of ferromagnetic exchange interactions within each of these chains. XAS measurements confirm the local coordination of the transition metal ions as well as their 2+ valence states. The transition metal ions in Cu_2CoSiO_5 (Cu_2NiSiO_5) start to order antiferromagnetically below about 15 K (12.5 K) with an incommensurate antiferromagnetic structure as revealed by polarized neutron scattering experiments on Cu_2CoSiO_5. The propagation vectors $\mathbf{k}^{\pm} = \pm(\sim 0.2\ 0\ 0.3)$ without components in the chain direction are also consistent with a ferromagnetic intrachain alignment of spins and a modulation between (and not within) these chains. Also the direction-dependent anisotropy of the size of the Curie-Weiss temperatures is consistent with a scenario where at least one of the Cu or Co chains exhibits ferromagnetic intrachain exchange interactions. Polarization analysis indicates magnetic moment directions perpendicular to the chains. Finally, Cu_2CoSiO_5 exhibits a large unquenched orbital moment of $\sim 1\,\mu_B$ size, as revealed by magnetic susceptibility measurements.

ACKNOWLEDGMENTS

The research in Dresden is supported by the Deutsche Forschungsgemeinschaft through Project No. 320571839. G.R. acknowledges the financial support by the National Research Foundation of Korea (NRF) funded by the Ministry of Science and ICT (No. 2016K1A4A4A01922028). We acknowledge support from the Max Planck-POSTECH-Hsinchu Center for Complex Phase Materials. We thank O. Stockert for helpful discussions.

[1] C. Naber, F. Goetz-Neunhoeffer, M. Göbbels, C. Rößler, and J. Neubauer, Cem. Concr. Res. **85**, 156 (2016).
[2] S. Jodlauk, P. Becker, J. A. Mydosh, D. I. Khomskii, T. Lorenz, S. V. Streltsov, D. C. Hezel, and L. Bohatý, J. Phys.: Condens. Matter **19**, 432201 (2007).
[3] M. Baum, A. C. Komarek, S. Holbein, M. T. Fernández-Díaz, G. André, A. Hiess, Y. Sidis, P. Steffens, P. Becker, L. Bohatý, and M. Braden, Phys. Rev. B **91**, 214415 (2015).
[4] W. Eerenstein, N. D. Mathur, and J. F. Scott, Nature (London) **442**, 759 (2006).
[5] S.-W. Cheong and M. Mostovoy, Nat. Mater. **6**, 13 (2007).
[6] L. Zhao, M. T. Fernández-Díaz, L. H. Tjeng, and A. C. Komarek, Sci. Adv. **2**, e1600353 (2016).
[7] J. R. Carvajal, Physica B **192**, 55 (1993).
[8] Y. Su, K. Nemkovskiy, and S. Demirdis, J. Large-Scale Res. Facil. **1**, A27 (2015).
[9] W. Schweika and P. Böni, Physica B **297**, 155 (2001).
[10] V. Petricek, M. Dusek, and L. Palatinus, *Structure Determination Software Programs* (Institute of Physics, Praha, Czech Republic, 2006).
[11] L. Palatinus and G. J. Chapuis, J. Appl. Crystallogr. **40**, 786 (2007).
[12] N. Hollmann, Z. Hu, M. Valldor, A. Maignan, A. Tanaka, H. H. Hsieh, H.-J. Lin, C. T. Chen, and L. H. Tjeng, Phys. Rev. B **80**, 085111 (2009).
[13] C. F. Chang, Z. Hu, H. Wu, T. Burnus, N. Hollmann, M. Benomar, T. Lorenz, A. Tanaka, H.-J. Lin, H. H. Hsieh, C. T. Chen, and L. H. Tjeng, Phys. Rev. Lett. **102**, 116401 (2009).
[14] T. Burnus, Z. Hu, H. Wu, J. C. Cezar, S. Niitaka, H. Takagi, C. F. Chang, N. B. Brookes, H.-J. Lin, L. Y. Jang, A. Tanaka, K. S. Liang, C. T. Chen, and L. H. Tjeng, Phys. Rev. B **77**, 205111 (2008).
[15] N. Hollmann, S. Agrestini, Z. Hu, Z. He, M. Schmidt, C.-Y. Kuo, M. Rotter, A. A. Nugroho, V. Sessi, A. Tanaka, N. B. Brookes, and L. H. Tjeng, Phys. Rev. B **89**, 201101(R) (2014).
[16] Q. Zhao, Y.-Y. Yin, J.-H. Dai, X. Shen, Z.-W. Hu, J.-Y. Yang, Q.-T. Wang, R.-C. Yu, Xi.-D. Li, and Y.-W. Long, Chin. Phys. B **25**, 020701 (2016).
[17] L. H. Tjeng, C. T. Chen, and S-W. Cheong, Phys. Rev. B **45**, 8205 (1992).
[18] J.-W. G. Bos, C. V. Colin, and T. T. M. Palstra, Phys. Rev. B **78**, 094416 (2008).
[19] F. Qian, L. J. Bannenberg, H. Wilhelm, G. Chaboussant, L. M. Debeer-Schmitt, M. P. Schmidt, A. Aqeel, T. T. M. Palstra, E. Brück, A. J. E. Lefering, C. Pappas, M. Mostovoy, and A. O. Leonov, Sci. Adv. **4**, eaat7323 (2018).
[20] S. Seki, X. Z. Yu, S. Ishiwata, and Y. Tokura, Science **336**, 198 (2012).
[21] A. Chacon, L. Heinen, M. Halder, A. Bauer, W. Simeth, S. Mühlbauer, H. Berger, M. Garst, A. Rosch, and C. Pfleiderer, Nat. Phys. **14**, 936 (2018).
[22] H. Effenberger and F. Pertlik, Monatsh. Chem. **117**, 887 (1986).